Punjab University Journal of Mathematics (2025), 57(05), 559-575
https://doi.org/10.52280/pujm.2025.57(05)04

Analytical Investigation of Casson Fluid Flow over a Riga Plate using the Prabhakar Fractional Derivative

*Khola Zainab
Department of Mathematics, University of Management and Technology, Lahore, Pakistan

Muhammad Abbas
Department of Mathematics, Riphah International University, Islamabad, Pakistan

Maria Haroon
Department of Mathematics, University of Management and Technology, Lahore, Pakistan

Muhammad Imran Asjad
Department of Mathematics, University of Management and Technology,Lahore, Pakistan
Center for Theoretical Physics, Khazar University, 41 Mehseti str., Baku, AZ1096, Azerbaijan

*Corresponding Author
kholazainab351@gmail.com

Received
10 February 2025

Accepted
05 September 2025

Published Online
13 November 2025

Abstract. This study analyzes unsteady Casson fluid flow over an accelerating Riga plate, utilizing Prabhakar fractional derivatives for stability analysis. Fourier and Fick's laws describe heat and mass transfer by capturing fluid-thermal-concentration relationships. The fractional PDEs are translated using the Laplace transform and solved analytically, with Zakian's numerical inversion applied to the velocity, temperature, and concentration fields. The effect of crucial parameters Casson number, Grashof numbers, Prandtl number, Hartmann number, fractional orders, magnetic and Schmidt numbers is investigated. The results provide light on flow stability and transport mechanisms, with important implications for engineering applications and future fractional calculus modeling of non-Newtonian fluid flows.

AMS (MOS) Subject Classification Codes: 35S29; 40S70; 25U09

Key Words: Casson fluid; Riga plate; Prabhakar fractional derivative; Zakian's algorithm; Laplace transform.

1. INTRODUCTION

Research projects are still being undertaken in the field of fluid dynamics in an effort to better understand the complexity of non-Newtonian fluid behavior. Two recent works have advanced this context, exploring different aspects of Casson fluid dynamics in different circumstances Khan et al. [16]. This work explores the fascinating field of Casson fluids in quadratically stratified and squeezed conditions, studying the flow properties when slip features are included over a surface that is heated convectively. The Casson model, or rheological model, was created by M. Hussain and Hayat et al. [12, 13] for suspending cylindrical particles. The distinctive method of simulating the flow behavior of non-Newtonian fluids, especially with regard to yield stress, sets Casson nanofluid rheology distinct from other nonlinear fluid models. Casson fluids have a nonlinear relationship between shear stress and shear rate, which is especially noticeable at low shear rates, in contrast to Newtonian fluids, which show a linear relationship Mahboobtosi et al. [20]. The industries of mineral extraction, material science, metallurgy, food manufacturing, and nanotechnology all have extensive real world uses for Casson flow. The relevance of Casson fluid in microchannels has recently attracted the attention of specialists due to computational and experimental studies of the fluid Abbas et al.[1,2] . Sene [29] developed a novel method for dealing with the fractional modified Casson flows model of the Caputo fractional operator. Arif et al. [6] thoroughly studied motor oil utilization, using a fractional mathematical model of Casson flows with rising wall temperature. Casson fluids are frequently investigated in industrial and biological applications because to their non-Newtonian behavior, such as yield stress and shear-thinning. This is relevant in flows including blood, drilling mud, coatings, lubricants, and sweet suspensions. Sohail et al. In electrically conducting Casson fluids under magnetic influence, Joule (ohmic) heating and viscous dissipation introduce important thermal effects that impact flow and heat transmission in high-shear or electrically driven systems [31]. Liu et al. [18] studied the effects of anomalous diffusion on an unsteady Casson fluid over a permeable medium. The study investigates the time-independent Casson fluid velocity over an exponentially infinite isothermal vertical permeable sheet Ali et al.[5]. These fluids find extensive use in numerous technical and engineering procedures, including those related to drilling mechanisms, food production, and extrusion processes.
Riga plate, propelled by technological progress, can be considered a fundamental element in the evolution of the engineering world. One external tool used to improve electrical conductivity is the Riga plate (RP). The electrodes and magnet pairs are arranged in a specific pattern on this plate. They demonstrated how the modified Hartmann number is suppressed as it rises in liquid temperature. The modified Hartmann number is used to determine whether or not the Riga plate is present. The authors emphasized that fluid velocity increases with the modified Hartmann number. Rizwana et al.[28] conducted a similar work that considered non-Newtonian nanofluid flow across an oscillating plate. In submarines, the Riga plate reduces drag force and friction by avoiding boundary layer separation and turbulence Daud et al. [9]. The Cattaneo-Christov heat flux model is used to calculate heat convection within a viscoelastic fluid induced by a stretching sheet by Reyaz et al. [25]. In the meantime, an investigation of the Riga plate over a heat-generating stratified Casson fluid and absorption was carried out by Loganathan and Deepa [19]. Using the implicit finite difference method, numerical solutions were achieved. As the modified Hartmann

number rises, the fluid velocity also increases, according to the findings. Consideration was taken into account rotational Casson fluid, Nasrin et al. [23] replicated the study, and their findings were consistent with those of Loganathan and Deepa. Concerning Riga plate studies, Mallawi et al. [21], Bhatti and Michaelides [8] , and Khatun et al.[17] are among the honorable mentions. Actuators known as riga plates are useful for regulating the velocity at which fluid flows. Investigating the properties of fluid flowing over Riga plates is worthwhile because they are frequently used in marine engineering.

Fourier's heat conduction law generally examines the majority of the features related to energy transfer. A number of researchers became interested in finding out how to increase the heat rate transfer. When it comes to classical heat transmission of fluids with low thermal conductivity, such as water, oil, and ethylene glycol, low heat transfer phenomena occur Shatanawi et al. [30]. For the same flux model, Ciarletta and Straughan also investigated the possibility of different stable solutions Reyaz et al. [26].

Fractional derivatives are a relatively recent addition to the field of fluid flow mechanics. Despite being purely theoretical, previous research has demonstrated that by incorporating fractional derivative into current engineering problems. Utilizing fractional order differential equations in mathematical modeling offers several benefits, most important of which is undoubtedly the non-local nature of these equations. It is imperative that is benefit be emphasized. It is well known that the differential operator for the whole order is a local operator and is a global for fractional orders Shaiq et at. [32]. The following are examples of fractional derivatives: the Liouville and Riemann-Liouville derivatives, the Caputo-Fabrizio derivative, the Prabhakar derivative, the Marchaud derivative, the Leibnitz derivative, the Grünwald-Letnikov derivative, the Caputo derivative, the Riesz derivative, the Hadamard derivative, and other mathematical operators Ahmed et al. [3]. The primary characteristics of the Prabhakar functions, also known as the three-parametric Mittag-Leffler functions Ahmed et al. [4] were introduced by Garra and Garrappa [10]. They also examined the thermal transport using Prabhakar memory. Giusti and Colombaro [11] recently conducted an analysis of a linear viscoelastic model is built on Prabhakar fractional operators. They devised a fractional generalized constitutive equation for Maxwell fluids that uses the Prabhakar derivative. They demonstrated the relationship within the concept of fractional integral operators with the Prabhakar kernel and the operator for differential developed by Caputo and Fabrizio. However, To find the mathematical solution of the created fractional model of temperature and velocity field, the Laplace transformation technique and some of its inverse methods, i.e. Zakians method, are used Raza et al. [24]. The Zakian approach was used to calculate the inverted Laplace transform of the velocity, concentration, and temperature distributions. The temperature and concentration profiles decrease more quickly as the values of the Schmidt, Prandtl, and Nb (Brownian motion parameters) increase. These patterns increase as a function of the temperatures and fractional components .

2. THE PROBLEM'S MATHEMATICAL EXPRESSION

Consider the heat energy transfer of a Casson flow across an permeable vertical Riga plate in the present of a constant magnetic field. When time $\tau = 0$, the plate and fluid are at rest and T'_∞ is temperature. The plate temperature increases to T'_w at $\tau > 0$ and

then remains constant. The plate starts to accelerate uniformly at $B\tau$,where B is the acceleration, when $\tau > 0$. When a penetrating homogeneous magnetic force is applied in a direction B_0 that is identical to the y-axis, the force flows. The created magnetic force has very little effect on the motion of fluids because of the low Reynolds number, which may be ignored. Only at $\zeta > 0$ is the y-coordinate, when measured orthogonal to the plate, taken into account. Then, it is maintained at that level
(Figure 1). Assumption made may be used to represent the isotropic Casson flow rheological equation of state [22, 15].

$$\tau = \mu\gamma + \tau_0$$
$$\tau_{ij} = \begin{cases} 2 \times (\mu_B + \frac{p_y}{2\pi})e_{ij} \ if \ \pi > \pi_c \\ 2 \times (\mu_B + \frac{p_y}{2\pi_c})e_{ij} \ if \ \pi_c > \pi \end{cases}$$

where π represents the rate of component deformation, π_c is the critical value, p_y is the fluid's yield stress, μ_B is the plastic dynamic fluid viscosity and here τ is the stress tensor.

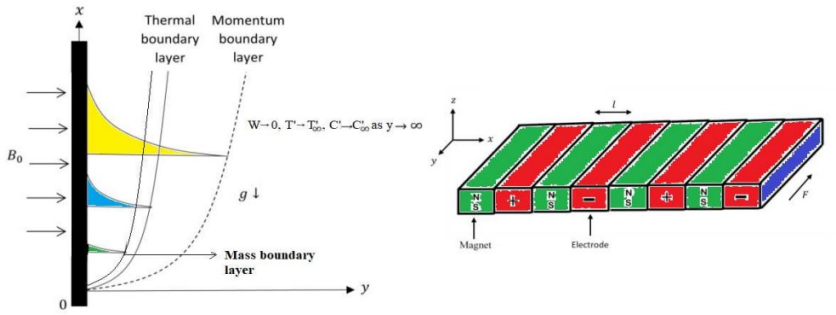

FIGURE 1. Flow Geometry

Using Boussinesq's approximation, the system under investigation produces the following Equations that regulate the Casson fluid flow [7,14].

$$\frac{\partial W(\xi,\tau)}{\partial \tau} = v(1+\frac{1}{\beta'})\frac{\partial^2 W(\xi,\tau)}{\partial \xi^2} + \frac{\pi J_0 M}{8\rho}\exp(-\frac{\pi}{l}\xi) + g\beta_T(T'-T'_\infty) + g\beta_c(C'-C'_\infty) \tag{2. 1}$$

Thermal equation

$$(\rho C_p)\frac{\partial T'}{\partial \tau} = -\frac{\partial q'}{\partial \xi} \tag{2. 2}$$

with Fourier's law for heat flux

$$q'(\xi,\tau) = -k\ {}^{C}D^{\gamma}_{\alpha,\beta,a}\frac{\partial T'(\xi,\tau)}{\partial \xi} \tag{2. 3}$$

Mass equation

$$\frac{\partial C'}{\partial \tau} = -\frac{\partial j'}{\partial \xi} \tag{2. 4}$$

with Fourier's law for mass flux

$$j' = D_m\ {}^{C}D^{\gamma}_{\alpha,\beta,a}\frac{\partial C'}{\partial \xi} \tag{2. 5}$$

and equations (1-5) are bounded by initial boundary conditions

$$W(\xi,0) = 0, \quad W(0,\tau) = B\tau, \quad W(\infty,\tau) \to 0, \tag{2. 6}$$

$$T'(\xi,0) = 0, \quad T'(0,\tau) = T'_w, \quad T'(\infty,\tau) \to T'_\infty, \tag{2. 7}$$

$$C'(\xi,0) = C'_\infty, \quad C'(0,\tau) = C'\tau, \quad C'(\infty,\tau) \to C'_\infty, \tag{2. 8}$$

where $\nu, \beta, \sigma, B_0, \rho, \beta_T, g, J_O, M, l, C_p, k$ are kinematic viscosity, Casson parameter, electrical conductivity, uniform magnetic field is, fluid density , electrical conductivity, uniform magnetic field, fluid density, volumetric thermal coefficient of expansion, gravitational force, current density, magnetisation of magnets is, width of electrodes and magnets, specific heat and heat conductivity parameter. By introducing the diemensionless variables

$$u^* = \frac{w}{(vB)^{\frac{1}{3}}}, \quad y^* = \frac{\xi B^{1/3}}{v^{2/3}}, \quad t^* = \frac{\tau B^{2/3}}{v^{1/3}}, \quad \theta = \frac{T'-T'_\infty}{T'_w-T'_\infty}, \quad \phi = \frac{C'-C'_\infty}{C'_w-C'_\infty},$$
$$j = \frac{j'}{j_0}; \quad j_0 = \frac{DB^{1/3}(C'_w-C'_\infty)}{v^{2/3}}, \quad q = \frac{q'}{q_0}; \quad q_0 = \frac{kB^{1/3}(T'_w-T'_\infty)}{v^{2/3}} \tag{2. 9}$$

and removing the star notations, we have dimensionless equations.

$$\frac{\partial u}{\partial t} = \frac{1}{\beta_0}\frac{\partial^2 u}{\partial y^2} + \frac{\pi J_0 M}{8\rho B}exp(-y\frac{\pi v^{2/3}}{lB^{1/3}}) + \theta Gr + \phi Gm. \tag{2. 10}$$

Thermal balance equation

$$Pr\frac{\partial \theta}{\partial t} = \frac{\partial q}{\partial y}, \tag{2. 11}$$

Fourier's law

$$q = -{}^{C}D^{\gamma}_{\alpha,\beta,a}\frac{\partial\theta}{\partial y}. \tag{2. 12}$$

Diffusion equilibrium formula

$$Sc\frac{\partial\phi}{\partial t} = \frac{\partial j}{\partial y}, \tag{2. 13}$$

Fick's principle

$$j = -{}^{C}D^{\gamma}_{\alpha,\beta,a}\frac{\partial\phi}{\partial y}. \tag{2. 14}$$

where,

$$L = \frac{\pi v^{2/3}}{lB^{1/3}}, \qquad Ha = \frac{\pi J_0 M}{8B\rho}, \qquad Gm = \frac{g\beta_c(C_w - C_\infty)}{B}, \qquad Gr = \frac{g\beta_T(T_w - T_\infty)}{B},$$

$$\beta_0 = \frac{\beta'}{\beta' + 1}, \quad Sc = \frac{v}{D}, \quad Pr = \frac{v_\rho C_P}{k},$$

where $L, Ha, Gm, Gr, \beta_0, Sc, Pr$ are constant parameter, Hartman number, mass Grashöf number, Grashöf number, Casson parameter, Schmidt number and Prandtl number with non-dimensional boundary conditions used here [27].

$$u(y,o) = 0, \quad u(0,t) = t, \quad u(\infty,t) \to 0, \tag{2. 15}$$

$$\theta(y,0) = 0, \quad \theta(0,t) = 1, \quad \theta(\infty,t) \to 0, \tag{2. 16}$$

$$\phi(y,0) = 0, \quad \phi(0,t) = 1, \quad \phi(\infty,t) \to 0. \tag{2. 17}$$

3. Prabhakar Fractional Derivative

$${}^{C}D^{\gamma}_{\alpha,\beta,a}g(t) = E^{-\gamma}_{\alpha,P-\beta,a}g^{(P)}(t) = e^{-\gamma}_{\alpha,P-\beta}\mathbf{(a;t)} * g^{(P)}(t) = \int_0^t (t-\tau)^{P-\beta-1}E^{-\gamma}_{\alpha,p-\beta}(a(t-\tau)^{\alpha})g^{(p)}(\tau)\,d\tau$$

$$E^{-\gamma}_{\alpha,\beta,a}g(z) = \int_0^t (t-\tau)^{P-\beta-1}E^{-\gamma}_{\alpha,\beta}(a(t-\tau)^{\alpha})g(\tau)\,d\tau$$

"*" is the the convolutional item, $g(p)$ symbolizes the pth derivative of $g(t)AC^{p}(0,b)$, (group of functions with real values) $g(t)$ whose derivatives keep going till $(p-1)$ order within the time frame $(0,b)$ where $g^{(p-1)}(t)$ is complete uninterrupted operation, and $p = [\beta]$ symbolizes the parameter's integer portion. β [33].

$$E^{\gamma}_{\alpha,\beta,a}g(t) = \int_0^t (t-\tau)^{\beta-1}E^{\gamma}_{\alpha,\beta}(a(t-\tau)^{\alpha})(\tau)\,d\tau$$

symbolizes the integral of Prabhakar and

$$E^{\gamma}_{\alpha,\beta,a}g(z) = \sum_0^{\infty}\frac{\Gamma(\gamma+n)z^n}{n!\Gamma(\gamma)\Gamma(\alpha n+\beta)}, \;\; \alpha,\beta,z \in C, \quad Re(\alpha) > 0$$

The Mittag-Leffler function has three parameters. This function has been defined..

$$e^{\gamma}_{\alpha,\beta}\mathbf{(a;t)} = t^{\beta-1}E^{\gamma}_{\alpha,\beta}(at^{\alpha}), \;\; t \in R, \alpha,\beta,\gamma,a \in C, \quad Re(\alpha) > 0$$

that called the kernel of Prabhakar. For standardized Prabhakar fractional derivatives, the Laplace transformation is supplied by

$$\begin{aligned}\mathbf{L}\{{}^{C}D^{\gamma}_{\alpha,\beta,a}g(t)\} = \mathbf{L}\{e^{-\gamma}_{\alpha,P-\beta,a}g^{(P)}(t)\} &= \mathbf{L}\{e^{-\gamma}_{\alpha,P-\beta,a}\}\mathbf{L}\{g^{(P)}(t)\} \\ &= s^{\beta-p}(1-as^{\alpha})\mathbf{L}\{g^{(p)}(t)\}\end{aligned} \tag{3. 18}$$

where,

$$h_p(\alpha,\beta,\gamma,a,t) = e^{-\gamma}_{\alpha,P-\beta}\textbf{(a; t)} \tag{3. 19}$$

is referred to as the regularized Prabhakar derivative's Prabhakar kernel.

4. Problem Solutions

4.1. **Temperature Equation.** Applying the Laplace transform and Prabhakar fractional derivative to Equations (11) and (12) with boundary conditions. The temperature field is

$$Pr\frac{\partial\theta}{\partial t} = \frac{\partial q}{\partial y}$$

Applying Laplace transformation

$$Prs\bar{\theta} = -\frac{\partial\bar{q}'(y,s)}{\partial y} \tag{4. 20}$$

$$q(y,t) = -{}^{C}D^{\gamma}_{\alpha,\beta,a}(\frac{\partial\theta}{\partial y})$$

Apply Laplace transformation

$$\bar{q}'(y,s) = -\mathbf{L}\{e^{-\gamma}_{\alpha,p-\beta}\textbf{(a;t)}(\frac{\partial\theta}{\partial y})^{p}(t)\}$$

$$\bar{q}'(y,s) = -s^{\beta-p}(1-as^{-\alpha})^{\gamma}\mathbf{L}\{(\frac{\partial\theta}{\partial y})^{p}(t)\}$$

where,

$$h_p(\alpha,\beta,\gamma,a,t) = e^{-\gamma}_{\alpha,p-\beta}(a;t)$$

is referred to as the regularized Prabhakar derivatives' Prabhakar kernel.

$$\bar{q}'(y,s) = -s^{\beta-p}(1-as^{-\alpha})^{\gamma}(\frac{\partial\bar{\theta}}{\partial y}) \tag{4. 21}$$

If we consider $\beta \in [0,1)$, Therefore, the parameter p is equal to zero. Furthermore, by using Laplace transform on Eq.(16), we get

$$\bar{\theta}(y,0) = 0, \quad \bar{\theta}(0,s) = \frac{1}{s} \tag{4. 22}$$

Introducing Eq.(21) into Eq.(20)

$$\frac{\partial^2\bar{\theta}}{\partial y^2} = \frac{Prs^{1-\beta}}{(1-as^{-\alpha})^{\gamma}}\bar{\theta}. \tag{4. 23}$$

Using Eq.(22) into Eq.(23). we get general solution

$$\bar{\theta}(y,s) = \frac{1}{s}exp(-y\sqrt{\frac{Prs^{1-\beta}}{(1-as^{-\alpha})^{\gamma}}}) \tag{4. 24}$$

Expand by exponentional series

$$\bar{\theta}(y,s)=\sum_{k=0}^{\infty}\frac{(Pr)^{\frac{k}{2}}(-y)^k s^{\frac{-\beta k}{2}+\frac{k-2}{2}}}{k!}(1-as^{-\alpha})^{-\gamma\frac{k}{2}} \tag{4. 25}$$

Applying Laplace inverse transformation

$$\theta(y,t)=\sum_{k=0}^{\infty}\frac{(-y)^k(Pr)^{\frac{k}{2}}}{k!}\mathbf{e}^{(\gamma\frac{k}{2})}_{\alpha,\frac{k}{2}(1-\beta)+1}\mathbf{(a;t)} \tag{4. 26}$$

4.2. **Concentration Equation.** Using the Prabhakar fractional derivative and Laplace transform on Eqs.(13) and(14) with boundary conditions. The concentration field is

$$Sc\frac{\partial\phi}{\partial t}=-\frac{\partial j(y,t)}{\partial y}$$

Applying Laplace transformation

$$Scs\bar{\phi}(y,s)=-[\frac{\partial\bar{j}'(y,t)}{\partial y}] \tag{4. 27}$$

$$j(y,t)=-{}^{C}D^{\gamma}_{\alpha,\beta,a}(\frac{\partial\phi}{\partial y})$$

by used Laplace transformation

$$j'(y,s)=-s^{\beta}(1-as^{-\alpha)^{\gamma}}\frac{\partial\bar{\phi}}{\partial y} \tag{4. 28}$$

Futhermore, by using the Laplace transform on Eq.(17), we have

$$\bar{\phi}(y,0)=0,\quad \bar{\phi}(0,s)=\frac{1}{s} \tag{4. 29}$$

Introducing Eq.(28) into Eq.(27)

$$\frac{\partial^2\bar{\phi}}{\partial y^2}=\frac{Scs^{1-\beta}}{(1-as^{-\alpha})^{\gamma}}\bar{\phi}(y,s) \tag{4. 30}$$

Using Eq.(29) in Eq.(30), we get the general solution as

$$\bar{\phi}(y,s)=\frac{1}{s}exp(-y\sqrt{\frac{Scs^{1-\beta}}{(1-as^{-\alpha})^{\gamma}}}) \tag{4. 31}$$

Expand by exponential series

$$\bar{\phi}(y,s)=\sum_{m=0}^{\infty}\frac{(-y)^m(Sc)^{\frac{m}{2}}s^{\frac{-\beta m}{2}+\frac{m-2}{2}}}{m!}(1-as^{-\alpha})^{-\gamma\frac{m}{2}} \tag{4. 32}$$

by used Laplace inverse transformation

$$\phi(y,t)=\sum_{m=0}^{\infty}\frac{(-y)^m(Sc)^{\frac{m}{2}}}{m!}\mathbf{e}^{(\gamma\frac{m}{2})}_{\alpha,1+(1-\beta)\frac{m}{2}}\mathbf{(a;t)} \tag{4. 33}$$

4.3. **Velocity Equation.** Taking Laplace transform of Eq.10

$$s\bar{u}(y,s) = \frac{1}{\beta_0}\frac{\partial^2 \bar{u}}{\partial y^2} + \frac{Ha}{s}exp(-yL) + Gr\bar{\theta}(y,s) + Gm\bar{\phi}(y,s) \tag{4. 34}$$

by Using Laplace transform on Eq.(15), we have

$$\bar{u}(y,o) = 0, \quad \bar{u}(0,s) = \frac{1}{s^2}. \tag{4. 35}$$

Rearrange of Eq.(34)

$$\frac{\partial^2 \bar{u}}{\partial y^2} - \beta_0 s\bar{u}(y,s) = -\frac{\beta_0}{s}Ha\, exp(-yL) - \beta_0 Gr\bar{\theta}(y,s) - \beta_0 Gm\bar{\phi}(y,s) \tag{4. 36}$$

Using Eq.(35) in Eq.(36), we get general solution as

$$\begin{aligned}\bar{u}(y,s) =& \frac{1}{s^2}exp(-y\sqrt{\beta_0 s}) + [\frac{\beta_0 Gr}{s[\frac{Prs^{1-\beta}}{(1-as^{-\alpha})^{\gamma}} - \beta_0 s]}][exp(-y\sqrt{\beta_0 s}) - exp(-y\sqrt{\frac{Prs^{1-\beta}}{(1-as^{-\alpha})^{\gamma}}})] \\ &+ [\frac{\beta_0 Gm}{s[\frac{Scs^{1-\beta}}{(1-as^{-\alpha})^{\gamma}} - \beta_0 s]}][exp(-y\sqrt{\beta_0 s}) - exp(-y\sqrt{\frac{Scs^{1-\beta}}{(1-as^{-\alpha})^{\gamma}}})] \\ &+ [\frac{\beta_0 Ha}{s(L^2 - \beta_0 s)}][exp(-y\sqrt{\beta_0 s}) - exp(-Ly)]\end{aligned} \tag{4. 37}$$

Using Zakian's procedure

$$f(t) = \frac{2}{t}\sum_{l=1}^{n} Re\{S_l F(\frac{\alpha_l}{t})\}, \tag{4. 38}$$

using the mentioned Eq.'s inverse Laplace transformation shape. The velocity area's final computation will be acquired.

5. Result and Discussion

The influence of the Riga plate and fractional parameter on the Casson flow on an infinite vertical plate is taken into account. In terms of the exponential function, the precise solutions for temperature and concentration are found.

5.1. **Graphs with Analysis for the Cason Fluid Model:** Consideration is given to how the Riga plate and fractional parameter affect the Casson flow on an infinite vertical plate. This section examines the behavior of the non-dimensional temperature, concentration, and velocity profiles for a range of fractional parameter values as well as the impact of additional physical elements. It enables us to investigate how the outcomes vary when fractional parameters are set to different values.

Figure 2 shows the relationship between fluid temperature and thermal fractional parameter, α, β, given fixed values for the remaining parameters. The temperature curve drops more sharply. When the plate cools, Figure 2 clearly shows that the temperature drops as the fractional parameter β rises. Figure 3 shows the effect of the third fractional parameter γ on the temperature field. The temperature decreases with the parameter γ, as this picture illustrates. Figure 4 shows the temperature profile decreases more rapidly with increasing

Prandtl number, indicating thinner thermal boundary layers. This is due to the reduced thermal diffusivity associated with higher Pr values.

Various values of the fractional parameter are represented in the concentration profile

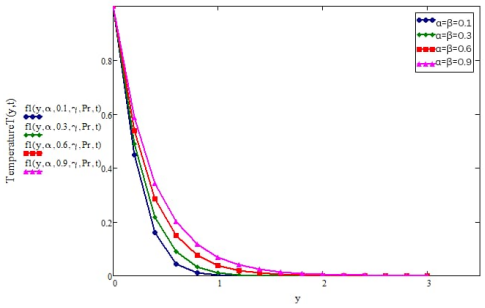

FIGURE 2. Effect of α, β on temperature profile

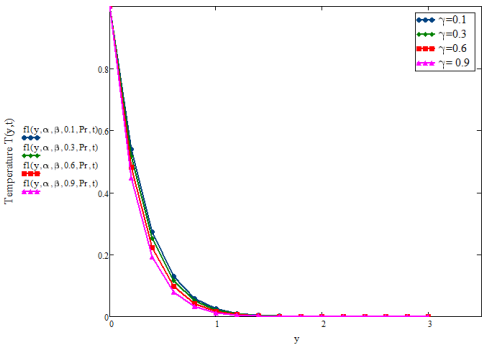

FIGURE 3. Effects of γ on temperature profile

in Figure 5. Concentration is dependent on viscosity, and viscosity increases with increasing Schmidt number. As α increases, the concentration decays faster. As β increases, concentration drops, and decay becomes steeper. A higher γ spreads the memory effect, causing a smoother and more sustained concentration profile. The effects of fractional parameters α, β, and γ on velocity profiles are depicted in Figure 6. It is observed that when these α grow at one specific moment, the time dependency of the Prabhakar fractional derivative's kernel causes velocity to decrease. Figure 7 shows Under the Prabhakar fractional derivative, higher fractional parameters intensify the flow velocity and extend the boundary layer. A greater Hartmann number (Ha) further amplifies the velocity relative to the non-magnetic condition. Figure 8 shows fluid velocity rising due to the rise of Gr. The Gr is a measure of the fluid's buoyant to viscous force relationship. Raising the value of Gr causes the fluid's buoyant force to increase, which in turn causes the fluid's vertical motion to increase. The fluid's velocity rises because it travels along the y-axis.

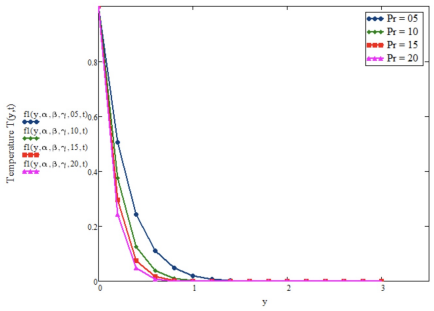

FIGURE 4. Effects of Pr on temperature profile

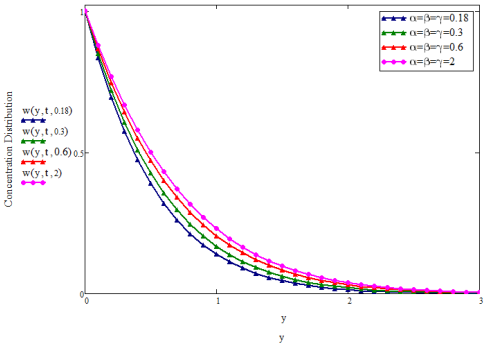

FIGURE 5. Effect of fractional parameters on concentration profile

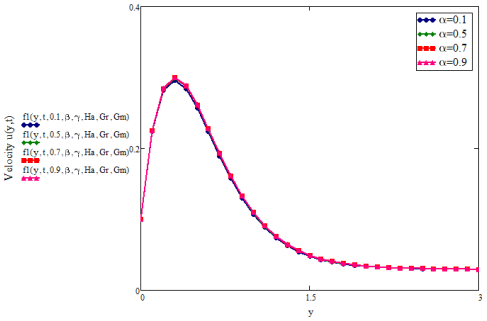

FIGURE 6. The velocity profile as affected by α

The effect of the Gm on the Casson fluid's velocity is shown in Figure 9. In the presence of the Riga plate, higher Hartmann number (Ha) and magnetic parameter (Gm) intensify the electromagnetic driving force, thereby enhancing velocity and thinning the boundary

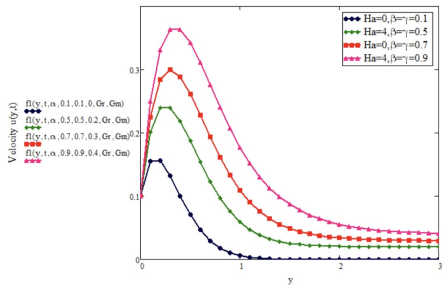

FIGURE 7. Influence of Ha, β and γ on velocity distribution with and without a Riga plate

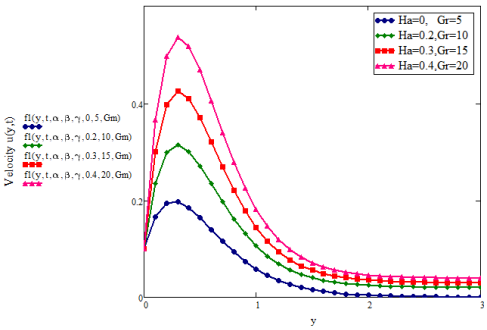

FIGURE 8. Influence of Ha and Gr on velocity profile in the presence and absence of the Riga plate

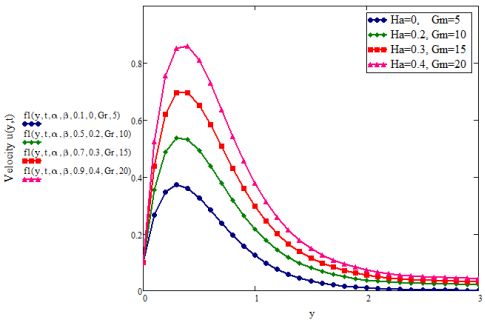

FIGURE 9. Influence of Ha and Gm on velocity profile in the presence and absence of the Riga plate

layer. In contrast, without the Riga plate, the same parameters act as resistive Lorentz forces, suppressing fluid motion. The Prabhakar fractional derivative further modulates these dynamics by introducing memory effects that prolong transient response Physically

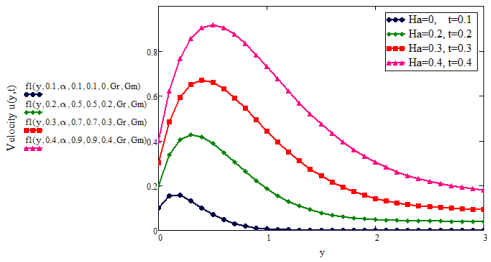

FIGURE 10. Influence of Ha and time on velocity profile in the presence and absence of the Riga plate

speaking, as Gm rises, buoyancy forces rise as increasing velocity. Figure 10 also shows the fluid's behavior as time t, increases values. These boundary value problems initial values would vary if the value of t changed. The velocity field governed by the Prabhakar fractional derivative shows notable amplification with increasing Hartmann number and time, signifying enhanced momentum transport. The generalized memory effects of the Prabhakar operator broaden the velocity boundary layer, highlighting its stronger dynamic influence compared to classical derivative. This is consistent with the fluid flow parameters established by equations (15-17). This study's findings are so applicable.

5.2. **Conclusion.** This paper explores the complex domain of fractional partial differential equations (PDEs) in the framework of Casson fluid dynamics. Selecting a mathematical model that meets theoretical expectations with experimental data can be done more effectively by using Prabhakar operators, particularly ones with specific fractional coefficients. The study uses graphical representations to clarify the physical consequences of different flow parameters, making use of the computational capability of the Mathcad application to provide a detailed knowledge of the underlying fluid dynamics.

i: The Grashöf number (Gr) effect on fluid velocity is also studied and it is reported that it is result contradictory and depends upon plate temperature. Cooling the plate is responsible for increasing fluid velocity and conversely heating the plate has a reverse consequence. This new discovery a great illustration of the effects of external perturbations on fluid dynamics - while it is a relatively small change, this subtlety is why a comprehensive mathematical model that accommodates these small features is so important. An increase in the Prandtl number (Pr) reduces both temperature and velocity profiles, as higher Pr limits thermal diffusion and results in a thinner thermal boundary layer. This suppression of heat transfer simultaneously weakens fluid motion through coupled thermal–momentum effects. These findings enrich the understanding of heat transfer mechanisms and offer valuable implications for thermal engineering applications.

ii: A key component of the research is the introduction of the Riga plate, which is shown to be effective in reducing turbulence effects and avoiding boundary layer separation. The plate's usefulness in lowering friction and pressure drag is further enhanced by its capacity

to generate electric and magnetic fields, which it can then divide and adhere to a flat surface, especially in underwater applications like submarines. The several functions of the Riga plate create opportunities for its integration into different engineering plans with the goal of maximizing fluid movement.

iii: One important use of the research is to simulate blood flow as a non-Newtonian fluid in veins and arteries. The analysis of fractional derivatives on the Riga plate using Casson fluid dynamics sheds light on blood flow behavior. The design and optimization of medical devices, such as artificial organs, catheters, and stents, could greatly benefit from this information. Contributing to the interdisciplinary subject of fluid biomechanics, the study bridges the gap between basic fluid dynamics and biomedical applications.

iv: An increase in the fractional parameters α, β, γ results in a decrease in velocity. Also fractional parameters reduce the temperature of the fluid.

v: By increasing the values of Pr temperature decrease.

v: The dynamic behavior of a Casson fluid over a Riga plate is revealed by the Prabhakar fractional derivative, underscoring the significance of fractional calculus in complex fluid analysis.

TABLE 1. Nomenclature

Symbol	Name	Unit
W	Fluid velocity	$[ms^{-1}]$
u	Fluid velocity	$[ms^{-1}]$
T'	Fluid temperature	$[K]$
C'	Concentration fluid	$[kgs^{-3}]$
C'_w	Concentration level at the plate	$[kgm^{-3}]$
C'_∞	Concentration away from the plate	$[kgs^{-3}]$
T'_w	Temperature of the fluid at the plat	$[K]$
T'_∞	Temperature of the fluid far from the plat	$[K]$
C_p	Specific heat at constant pressure	$[Jkg^{-1}K^{-1}]$
D	Mass diffusivity	$[m^2s^{-1}]$
g	Acceleration due to gravity	$[ms^{-2}]$
k	Thermal conductivity of fluid	$[Wm^{-1}K^{-1}]$
ν	Fluid Kinematic viscosity	$[ms^{-2}]$
μ	dynamic viscosity	$[kgm^{-1}s^{-1}]$
ρ	Density fluid	$[kgm^{-3}]$
t	Time	[s]
β_T	Thermal expansion for volumetric coefficient	$[K^{-1}]$
β_C	volumetric coefficient of mass expansion	$[m^3Kg^{-1}]$
β, γ	Fractional parameters	(-)
M	Magnetic parameter	(-)
s	Laplace transform variables	(-)
B_0	Uniform applied magnetic field	(-)
σ	electrical conductivity	(-)
j_0	current density	(-)

Conflict of Interest: The authors declare that they have no conflict of interest.

Funding Statement: No specific funding is available.

Ethics Approval and Consent to Participate: All the authors approve their consent.

Availability of Data and Materials: All data analyzed during this study are included in this published article.

Consent for Publication: All the authors approve this version for publication.

REFERENCES

[1] S. Abbas, M. Ahmad, A. A. Rahimzai, M. Nazar, and I. Khan, Active and passive control of MHD Jeffrey nanofluid over a vertical plate with constant proportional Caputo fractional derivative, (2023).

[2] S. Abbas, Z. U. Nisa, M. Nazar, M. Amjad, H. Ali, and A. Z. Jan, Application of heat and mass transfer to convective flow of Casson fluids in a microchannel with Caputo–Fabrizio derivative approach, Arab. J. Sci. Eng. **49**, No. 1 (2024) 1275–1286.

[3] N. Ahmed, D. Vieru, C. Fetecau, and N. A. Shah, Convective flows of generalized time-nonlocal nanofluids through a vertical rectangular channel, Phys. Fluids **30**, No. 5 (2018) 053102.

[4] N. Ahmed, N. A. Shah, B. Ahmad, S. I. A. Shah, S. Ulhaq, and M. Rahimi Gorji, Transient MHD convective flow of fractional nanofluid between vertical plates, J. Appl. Comput. Mech. **5**, No. 4 (2019) 592–602.

[5] F. Ali, A. Zaib, M. Khalid, T. Padmavathi, B. Hemalatha, Unsteady MHD flow of Casson fluid past vertical surface using Laplace transform solution, J. Comput. Biophys. Chem. **22**, No. 3, (2023) 361–37.

[6] M. Arif, P. Kumam, W. Kumam, I. Khan, and M. Ramzan, A fractional model of Casson fluid with ramped wall temperature: engineering applications of engine oil, Comput. Math. Methods **3,** No. 6 (2021) e1162.

[7] M. I. Asjad, P. Sunthrayuth, M. D. Ikram, T. Muhammad, and A. S. Alshomrani, Analysis of non-singular fractional bioconvection and thermal memory with generalized Mittag–Leffler kernel, Chaos Solitons Fractals **159** (2022) 112090.

[8] M. Bhatti and E. E. Michaelides, Study of Arrhenius activation energy on the thermo-bioconvection nanofluid flow over a Riga plate, J. Therm. Anal. Calorim. 143 (2021) 2029–2038.

[9] M. M. Daud, L. Y. Jiann, R. Mahat, S. Shafie, Application of Caputo fractional derivatives to the convective flow of Casson fluids in a microchannel with thermal radiation, J. Adv. Res. Fluid Mech. Therm. Sci. **93**, No. 1 (2022) 50–63.

[10] R. Garra and R. Garrappa, The Prabhakar or three-parameter Mittag–Leffler function: theory and application, Commun. Nonlinear Sci. Numer. Simul. **56** (2018) 314–329.

[11] A. Giusti and I. Colombaro, Prabhakar-like fractional viscoelasticity, Commun. Nonlinear Sci. Numer. Simul. **56** (2018) 138–143.

[12] T. Hayat, S. A. Khan, and S. Momani, Finite difference analysis for entropy optimized flow of Casson fluid with thermo-diffusion and diffusion-thermo effects, Int. J. Hydrogen Energy **47**, No. 12 (2022) 8048–8059.

[13] M. Hussain, A. Ghaffar, A. Ali, A. Shahzad, K. S. Nisar, M. Alharthi, and W. Jamshed, MHD thermal boundary layer flow of a Casson fluid over a penetrable stretching wedge in the existence of nonlinear radiation and convective boundary condition, Alex. Eng. J. **60**, No. 6 (2021) 5473–5483.

[14] M. Imran, N. A. Shah, I. Khan, and M. Aleem, Applications of non-integer Caputo time fractional derivatives to natural convection flow subject to arbitrary velocity and Newtonian heating, Neural Comput. Appl. **30**, No. 5 (2018) 1589–1599.

[15] A. Khalid, I. Khan, S. Shafie, Exact solutions for unsteady free convection flow of Casson fluid over an oscillating vertical plate with constant wall temperature, Abstr. Appl. Anal. **2015**, No. 1 (2015) 1–8.

[16] Q. Khan, M. Farooq, S. Ahmad, S. B. Moussa, Investigation of quadratically stratified squeezed Casson fluid flow with slip features over a convectively heated surface, Materials Sci. Eng. B **294**, No. **3** (2023) 116518.

[17] S. Khatun, M. M. Islam, M. T. Mollah, S. Poddar, and M. M. Alam, EMHD radiating fluid flow along a vertical Riga plate with suction in a rotating system, SN Appl. Sci. **3** (2021) 1–14.

[18] C. Liu, L. Zheng, P. Lin, M. Pan, F. Liu, Anomalous diffusion in rotating Casson fluid through a porous medium, Physica A **528**, No. 1 (2019) 121431.

[19] P. Loganathan and K. Deepa, Stratified Casson fluid flow past a Riga plate with generative/destructive heat energy, Int. J. Appl. Comput. Math. **6** (2020) 1–20.

[20] M. Mahboobtosi, B. Jalili, A. Shateri, P. Jalili, and D. D. Ganji, Heat transfer characteristics in the squeezing flow of Casson fluid between circular plates: A comprehensive study, Adv. Mech. Eng. **16**, No. 10 (2024) 16878132241290942.

[21] F. Mallawi, M. Bhuvaneswari, S. Sivasankaran, and S. Eswaramoorthi, Impact of double-stratification on convective flow of a non-Newtonian liquid in a Riga plate with Cattaneo–Christov double-flux and thermal radiation, Ain Shams Eng. J. **12**, No. 1 (2021) 969–981.

[22] S. Mukhopadhyay, Effects of thermal radiation on Casson fluid flow and heat transfer over an unsteady stretching surface subjected to suction/blowing, Chin. Phys. B **22**, No. 11 (2013) 114702.

[23] S. Nasrin, R. N. Mondal, and M. M. Alam, Impulsively started horizontal Riga plate embedded in unsteady Casson fluid flow with rotation, J. Appl. Math. Phys. **8**, No. 9 (2020) 1861–1876.

[24] A. Raza, I. Khan, S. Farid, C. A. My, A. Khan, and H. Alotaibi, Non-singular fractional approach for natural convection nanofluid with damped thermal analysis and radiation, Case Stud. Therm. Eng. **28** (2021) 101373.

[25] R. Reyaz, A. Q. Mohamad, Y. J. Lim, S. Shafie, Analytical solutions for fractional Caputo–Fabrizio Casson nanofluid on Riga plate with Newtonian heating, J. Adv. Res. Appl. Sci. Eng. Technol. **29**, No. 1 (2022) 142–159.

[26] R. Reyaz, A. Q. Mohamad, L. Y. Jiann, M. Saqib, and S. Shafie, Presence of Riga plate on MHD Caputo Casson fluid: an analytical study, J. Adv. Res. Fluid Mech. Therm. Sci. 93, No. 2 (2022) 86–99.

[27] R. Reyaz, A. Q. Mohamad, L. Y. Jiann, S. Shafie, Analytical treatment for accelerated Riga plate on fractional Caputo–Fabrizio Casson fluid, CFD Lett. **15**, No. 4 (2023) 114–123.

[28] R. Rizwana, S. Nadeem, et al., Series solution of unsteady MHD oblique stagnation point flow of copper-water nanofluid flow towards Riga plate, Heliyon **6**, No. 10 (2020) e05122.

[29] N. Sene, A new approach for the solutions of the fractional generalized Casson fluid model described by Caputo fractional operator, Adv. Theory Nonlinear Anal. Appl. **4**, No. 4 (2020) 373–384.

[30] W. Shatanawi, N. Abbas, T. A. Shatnawi, and F. Hasan, Heat and mass transfer of generalized Fourier and Fick's law for second-grade fluid flow at slendering vertical Riga sheet, Heliyon **9**, No. 3 (2023) e14248.

[31] M. Sohail, Y.-M. Chu, E. R. El-Zahar, U. Nazir, T. Naseem, Contribution of joule heating and viscous dissipation on three dimensional flow of Casson model comprising temperature dependent conductance utilizing shooting method, Phys. Scr. **96**, No. 8 (2021) 085208.

[32] M. S. Shaiq, S. Ali, A. Shahzad, T. Naseem, Time-Fractional Navier–Stokes Equation Solved by Fractional Variation of Parameters Method: An Analytic Approach, Int. J. Emerg. Multidiscip. Math. **2**, No. 1 (2023) 1–8.

[33] Y.-L. Sun, N. A. Shah, Z. A. Khan, Y. M. Mahrous, B. Ahmad, J. D. Chung, and M. N. Khan, Exact solutions for natural convection flows of generalized Brinkman type fluids: A Prabhakar-like fractional model with generalized thermal transport, Case Stud. Therm. Eng. 26 (2021) 101126.